# Particle dynamics in a turbulent electric field

A. Guillevic, M. Lesur, X. Garbet, P. Diamond, G. Lo-Cascio, Y. Kosuga, E. Gravier, D. Mandal, A. Ghizzo, T. Réveillé

RESEARCH ARTICLE | MAY 01 2023

# Particle dynamics in a turbulent electric field

A. Guillevic ; M. Lesur ; X. Garbet ; P. Diamond ; G. Lo-Cascio ; Y. Kosuga ; E. Gravier ; D. Mandal ; A. Ghizzo ; T. Réveillé



*Phys. Plasmas* 30, 052301 (2023)
https://doi.org/10.1063/5.0135918

Physics of Plasmas ARTICLE scitation.org/journal/php

# Particle dynamics in a turbulent electric field

Cite as: Phys. Plasmas **30**, 052301 (2023); doi: 10.1063/5.0135918
Submitted: 23 November 2022 · Accepted: 13 April 2023 ·
Published Online: 1 May 2023



A. Guillevic,[1,a)] M. Lesur,[1] X. Garbet,[2] P. Diamond,[3] G. Lo-Cascio,[1] Y. Kosuga,[4] E. Gravier,[1] D. Mandal,[1] A. Ghizzo,[1] and T. Réveillé[1]

## AFFILIATIONS

[1]Université de Lorraine, CNRS - IJL, F-54000 Nancy, France
[2]CEA, IRFM, F-13108 Saint-Paul-lez-Durance, France
[3]CASS, University of California San Diego, 9500 Gilman Dr, La Jolla, California 92093, USA
[4]Research Institute for Applied Mechanics, Kyushu University, Kasuga-kouen 6-1, Kasuga, Fukuoka 819-0395, Japan

[a)]**Author to whom any correspondence should be addressed:** alejandro.guillevic@univ-lorraine.fr

## ABSTRACT

Charged particle velocity-space diffusion in a prescribed one-dimensional turbulent electric field is investigated through numerical trajectories in phase-space and compared against quasi-linear theory (QL), including resonance broadening (RB). A Gaussian spectrum electric field of variable amplitude $E$ is studied in conjunction with two plasma dispersion relations, namely, the Langmuir and ion-acoustic dispersion. A first parameter scan shows that RB effects become significant for a Kubo number $K$ of a few percent. A Kubo number scan shows that diffusion increases as a power law of $D \propto K^3 \propto E^{3/2}$ for large Kubo numbers. Moreover, at large Kubo numbers, transport processes include significant diffusion measured at velocities much higher than the resonant region, where QL and RB predict negligible diffusion. For times much larger than the trapped particle flight time $\tau_b$ and the autocorrelation time $\tau_0$, the velocity distribution departs from a Gaussian. Nevertheless, measurements show that the variance increases linearly in time, with a Hurst parameter of $H \sim 0.5$, where the diffusion scales as $K^{5/2} \propto E^{5/4}$ and $K^{3/2} \propto E^{3/4}$ for small and large Kubo number, respectively.





## I. INTRODUCTION

The full description of charged particle dynamics in an electric field including several waves is sometimes divided into two categories: First, in the small amplitude limit, each particle interacts linearly with only one of the waves, and the dynamics are regular. Second, as the amplitude of the waves grows, particles interact with more than one wave leading to chaotic dynamics. From the point of view of the waves, the non-linear wave–particle interactions lead to energy cascades from one wave toward many other waves,[1] leading to the generation of lower and higher modes; here, the modes refer to the eigenfunction of the system. In fully developed turbulence, the electric field modes can be in random phase between each other, and the dynamics become complex; particles can be trapped in a wave and again de-trapped due to the interaction of a different mode. In a collision-less plasma, turbulence is one of the leading causes of particle transport and energy losses through plasma wave–particle resonances. In addition, a significant impact of turbulence is in the heating of the plasma in the form of particle acceleration.[2] The heating of particles has substantial consequences when energetic particles drive instabilities in magnetic reconnection in space plasmas,[3,4] stimulated Raman scattering,[5] or laser–plasma interactions.[6]

In the early 60s, turbulence studies saw a surge with the introduction of quasi-linear theory[7–9] and resonance broadening.[10,11] Quasi-linear theory first aimed to study the problem of plasma dynamics outside equilibrium by neglecting mode coupling, considering part of the non-linear terms, and the evolution in time of particle distribution, in which it is assumed that turbulence does not trap particles. Under these conditions, it is possible to derive an expression for transport as an expansion of the electric field amplitude. For moderate amplitudes (or low dispersion), non-linear terms are no longer negligible, which leads to a broadening of wave–particle resonances and mode coupling effects. Including the effect of QL diffusion in the model of particle motion, known as re-normalization, enables the account of this broadening.[12,13]

For prescribed electric fields with random phases, studies have shown a strong qualitative and quantitative agreement with the quasi-linear theory[14,15] at low electric field amplitude. Here, we investigate the effects of high amplitude turbulence.[16–18] Regarding the self-consistent problem that is accounting for the modification of mean fields, it has been experimentally[19–21] and numerically[22] demonstrated that re-normalization is not necessary at low amplitude. Nevertheless, recent numerical simulations for the self-consistent bump-on-tail

instability[23] reveal that the quasi-linear theory fails to predict plasma processes at low amplitude, enhanced diffusivity, and phase-space restructuring.

Analytically, one of the parameters ruling the validity of quasi-linear and resonance-broadening theories is measured in terms of the Kubo number.[24] This quantity is defined as the ratio between the time it takes the turbulent electric field to change its shape, referred to as the autocorrelation time $\tau_0$, and the time it takes a trapped particle to complete an orbit, referred to as the flight time or bounce time $\tau_b$. In other words, the Kubo number is

$$K = \tau_0/\tau_b. \tag{1}$$

Alternatively, by rewriting this expression as a function of the electric field amplitude, we obtain the expression $K \propto E^{1/2}$, since $\tau_b \propto E^{-1/2}$. Note that, for quasi-linear and resonance broadening theories to be applied, the Kubo number should be much lower than unity $K \ll 1$.[9]

The importance of the Kubo number is ubiquitous in the literature related to turbulence. First, it allows the differentiation of the type of trajectory performed. As a mental representation, one may picture particles jumping between arcs of trapped trajectories for $K \ll 1$ and particles performing multiple trapped orbits separated by small jumps (or arcs) between two different trapped particle trajectories[25,26] for $K \geq 1$. Furthermore, the Kubo number emerges in multiple plasma turbulence theories, such as quasi-linear and mean-field theories,[27–29] the latter describing the relaxation transport in plasmas.

Calculations based on mixing length theory assume that the Kubo number is close to unity $K \simeq 1$,[27,30] rather than $K \ll 1$, as required for the validity of the quasi-linear theory. However, mixing-length and quasi-linear theories are often used simultaneously.

This study investigates the statistical diffusion coefficient of test particles in a prescribed one-dimensional turbulent electric field. We compare results from numerical trajectories against quasi-linear theory, including resonance broadening. Diffusion is investigated for ion-acoustic and Langmuir dispersion relations to compare the effects of dispersivity, and a Gaussian amplitude electric potential spectrum is adopted. Different regimes of particle trapping[14,15] are investigated, $K \geq 1$ in particular. We address the following questions: How far quasi-linear theory works from the $K \ll 1$ regime? Is there a way to expand, correct, or replace quasi-linear theory to describe a plasma in the $K > 1$ regime? These questions are deeply connected with standard map problem.[31–34] In this work, we are concerned with many resonances.

In Sec. II, quasi-linear and resonance-broadening theories are presented. We introduce the analytical description for the prescribed electric field in Sec. III in the case of plasma waves. Numerical results are reported in Secs. III B and III C for small and large Kubo number regimes, respectively. Finally, a conclusion is provided in Sec. IV.

## II. TURBULENT AUTOCORRELATION TIME AND QUASI-LINEAR THEORY

In this section, we introduce the quasi-linear theory[9,35] and resonance broadening correction[10,12,36,37] to study homogeneous steady-state turbulence in a one-dimensional plasma.

### A. Autocorrelation time

We focus on the Eulerian two-point autocorrelation function of the electric field $E(x, t)$, defined as $\langle E(0,0)E(x,t)\rangle$, where the brackets $\langle\cdot\rangle$ stand for the statistical average over an ensemble of particles whereas $t$ and $x$ are the displacements over time and space, respectively.

From the point of view of a particle at a given velocity $v$, the electric field evolves over a characteristic timescale called autocorrelation time. This time defines the typical time over which there is a noticeable change in the electric field shape. Analytically, the Lagrangian autocorrelation time $\tau_0(v)$[24] is defined as the integral of the two-point autocorrelation of the electric field

$$\tau_0(v) = \frac{1}{\langle E(0,0)^2\rangle}\int_0^{+\infty} dt \int_{-\infty}^{+\infty} dx \delta(x - vt)\langle E(0,0)E(x,t)\rangle, \tag{2}$$

where $\delta(x - vt)$ is the Dirac delta function and $v$ is the velocity of particles in the electric field. By solving the space, integral equation (2) is simplified as

$$\tau_0(v) = \frac{1}{\langle E(0,0)^2\rangle}\int_0^{+\infty} dt \langle E(0,0)E(vt,t)\rangle. \tag{3}$$

Note that $\tau_0$ is often interpreted as the time it takes for the electric field to change its shape. However, for our purposes, it represents the time it takes particles to receive a velocity kick from a low-amplitude turbulent electric field, in other words, $K \ll 1$.

### B. Quasi-linear theory for low amplitude fields

To study the one-dimensional motion $[x_i(t), v_i(t)]$ of a charged particle, identified by an index $i$, in a turbulent electric field $E(x, t)$, we use Newton's equation of motion

$$\frac{d^2x_i}{dt^2} = \frac{q}{m}E(x_i, t), \tag{4}$$

where $q$ and $m$ are the electric charge and mass of the particle, respectively.

By integrating equation of motion (4) over time, the $i$th particle velocity variation $\Delta v_i(t) = v_i(t) - v_i(0)$ at time $t$ is obtained as

$$\Delta v_i(t) = \frac{q}{m}\int_0^t dt' E(x(t'), t'). \tag{5}$$

Moreover, the statistical mean square variation $\sigma_v^2$, or variance, of an ensemble of $N$ particles is defined as

$$\sigma_v^2 = \frac{1}{N}\sum_{i=1}^{N}(\Delta v_i(t))^2. \tag{6}$$

In quasi-linear theory, the unperturbed motion $x_i(t) = x_i(0) + v_i t$ is substituted into Eqs. (5) and (6). Then, by considering that the electric field evolves slowly in time, we can simplify the double integral in the square term of (6) to a single integral in time. For large enough times, it becomes

$$\sigma_v^2 = 2tD_0(v). \tag{7}$$

Reminiscent of Brownian motion, the velocity variance increases linearly with time. Here, the rate of increase is given by the following quasi-linear diffusion coefficient:

$$D_0(v) = \frac{q^2}{m^2}\langle E(0,0)^2\rangle\tau_0(v), \tag{8}$$

which is proportional to the autocorrelation time defined in Eq. (2), and the intensity $\langle E(0,0)^2 \rangle$ of the turbulent field for $K \ll 1$, or by using expression (1), becomes a function of the Kubo number. Contrary to Brownian motion, where diffusion occurs in the real space $x$, diffusion of charged particles in a $1D$ turbulent electric field occurs in the velocity space $v$.

### C. Resonance broadening

The diffusion coefficient $D_0$, as given in Eq. (8), depends on two parameters: the amplitude of the electric field and the velocity of the particle trajectories. As the amplitude of the field increases, the assumption of an unperturbed motion is no longer valid. The number of modes able to interact strongly with the particle increases, leading to more complex dynamics. However, interactions between particles and waves remain local, in the sense that only waves in a range $\Delta v = (D_0(v)/k(v))^{1/3}$ about $v$ induce chaotic diffusion, while the other ones act perturbatively.[10,38] This locality can help to understand intuitively that the diffusion picture remains valid for moderate amplitude.[39] The widening of the resonant region is considered in resonance broadening theory.[10,15,37]

To account for this widening of resonance region and correct the diffusion coefficient, resonance broadening theory[14] suggests computing the diffusion coefficient through an iterative procedure. At step $n$, the diffusion coefficient calculated in the previous step $n-1$ is used to calculate a broadening probability distribution

$$P_{n-1}(v,x,t) = \left[2\pi\sigma^2_{x,n-1}\right]^{-1/2} \exp\left[-\frac{(x-vt)^2}{2\sigma^2_{x,n-1}}\right], \tag{9}$$

which substitutes the Dirac distribution function in Eq. (2). The position standard deviation $\sigma^2_{x,n-1}$ at the $n-1$ iteration is defined by

$$\sigma^2_{x,n-1} = \frac{2}{3} t^p D^{RB}_{n-1}(v), \tag{10}$$

where $D^{RB}_{n-1}$ is the resonance-broadening diffusion coefficient defined in Eq. (11) and $p \in ]2,4[$ is a real number that gives the time-dependence of the position standard deviation. The value of this parameter is discussed in Sec. III B and Subsec. 1 of Appendix B.

This procedure yields the resonance broadening diffusion coefficient at step $n$ from the point of view of particles initially at $v$

$$D^{RB}_n(v) = \frac{q^2}{m^2} \int_0^{+\infty} dt \int_{-\infty}^{+\infty} dx P_{n-1}(v,x,t) \langle E(0,0)E(x,t) \rangle. \tag{11}$$

At step $n=1$, $D^{RB}_0(v) = D_0(v)$ is calculated in Eq. (8) from linear orbits. This iterative method converges rapidly (typically in a few iterations) toward a resonant broadening diffusion coefficient $D^{RB}_\infty(v)$.

In resonance broadening, the characteristic time $\tau_{RB}$[10,39,40] is defined as

$$\tau_{RB} \sim \left(\frac{k^2 D_0}{6}\right)^{-1/3} \propto K^{-4/3}, \tag{12}$$

where $D_0$ is the quasi-linear regime diffusion coefficient and $k$ is the resonant wave number.

Note that if the autocorrelation function is given, one can solve the quasi-linear diffusion (8), and resonance broadening diffusion (11). However, when the autocorrelation is not analytical, one can solve these equations in Fourier space. Indeed, since we study homogeneous steady-state turbulence, and particle trajectories are well inside the chaotic domain, then Boltzmann's ergodic hypothesis[41] tells us that ensemble and space averaging are equal $\langle \cdot \rangle = \langle \cdot \rangle_x$.[42] Consequently, one can solve this equation by transforming the autocorrelation to a sum over the wavenumber $k$ using a Fourier transformation of the electric field $E(x,v)$ and Parseval's identity to solve the space integral. Therefore, after a few calculations, Eqs. (8) and (11) become, respectively,

$$D_0(v) = \frac{q^2}{m^2} \int_0^{+\infty} dt \sum_k \frac{\hat{E}_k^{\,2}}{2} \cos\left[(kv-\omega)t\right], \tag{13}$$

$$D^{RB}_n(v) = \frac{q^2}{m^2} \int_0^{+\infty} dt \sum_k \frac{\hat{E}_k^{\,2}}{2} e^{-\frac{\sigma^2_{x,n-1}k^2}{2}} \cos\left[(kv+\omega)t\right], \tag{14}$$

where the integrand in Eq. (13) corresponds to the autocorrelation function of the electric field $\langle E(0,0)E(x,t) \rangle$, the integrand in Eq. (3). First note that Eqs. (13) and (14) look similar except for a coefficient and sign difference in the cosine term. Indeed, the coefficient corresponds to the Fourier transform of the probability distribution $P_{n-1}$ from Eq. (9), and the sign in front of $\omega$ appears as the space integral is developed, and by assuming a symmetric dispersion relation, one can show in the QL limit that Eq. (14) becomes Eq. (13).

## III. APPLICATION TO PLASMA WAVES

Generally, when studying plasmas, a kinetic approach is preferred. In this case, the electric field and distribution function are solved simultaneously through the self-consistent Vlasov–Poisson system. However, this study focuses on the effects of a prescribed turbulent electric field on particle dynamics. Therefore, a test particle approach is preferred. Note that this approach is simpler than the self-consistent problem that led to the development of QL theory; nevertheless, quality information can be gathered through this method.

### A. Dispersion relation and amplitude electric field

For one-dimensional plasma, two ubiquitous waves are the Langmuir plasma wave and ion-acoustic wave (IA). Their respective dispersion relations are

$$\omega^L(k) = \sqrt{\omega_p^2 + 3v_{th}^2 k^2}, \tag{15}$$

$$\omega^{IA}(k) = \sqrt{\frac{c_s^2 k^2}{1+\lambda_D^2 k^2}}, \tag{16}$$

where $\omega_p$, $\lambda_D$, and $c_s$ are the electron plasma frequency, Debye length, and ion sound velocity, respectively. We choose to study both Langmuir and ion-acoustic waves since they have qualitatively distinct properties regarding the evolution of frequency (constant for small $k$ and linear for large $k$ for Langmuir and opposite for ion-acoustic waves), resulting in a broad vision of the phenomena present in a one-dimensional plasma.

In this paper, we chose a simple Gaussian amplitude spectrum $\hat{E}_k^{\,G}(k)$[14] defined as

$$\hat{E}_k^{\,G}(k) = k a_0 \sqrt{\frac{2}{\delta k \sqrt{\pi}}} \exp\left[-\left(\frac{k-k_0}{2\delta k}\right)^2\right], \tag{17}$$

where $k_0$, $\delta k^2$, and $a_0$ are the mean wavenumber, variance, and amplitude of the electric field spectrum, respectively. Figure 1 shows the

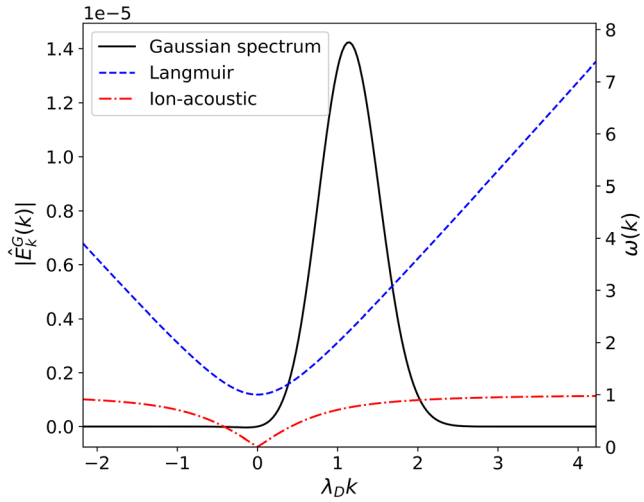


**FIG. 1.** Turbulent electric field characteristics: In solid line wave number spectrum from Eq. (17), in blue dashed line the Langmuir wave dispersion relation, and in red dash-dotted the ion-acoustic wave dispersion relation, with arbitrary amplitude $a_0$ and parameters $\lambda_D k_0 = 1$, $\lambda_D \delta k = 0.4$.

typical dispersion relation functions and Gaussian spectrum of arbitrary amplitude, used in this paper as a function of the wavenumber $k$.

### B. Case of Gaussian spectrum, small Kubo number

The numerical study of test particle trajectories requires us to prescribe a "turbulent" electric field. In other words, the modes of the electric field have random phases. In this paper, the electric field is chosen to be a sum of $M$ sinusoidal modes with random phases, defined as

$$E(x,t) = \sum_{j=1}^{M} \hat{E}_k^{\,G} \sin(\omega_j t - k_j x + \beta_j), \tag{18}$$

where $k_j$ is the wave number distributed uniformly between $[-2.2, 4.2]$ the standard deviation of the $k$ distribution $\delta_k = 0.4$ and the mean $k_0 = 1$, all in units of $\lambda_D$. $\omega_j$ is the frequency from Eqs. (15) and (16), and $\beta_j$ is the initial random phase uniformly distributed between $[0, 2\pi[$ of the $j$th mode. $\hat{E}_k^{\,G}$ is the amplitude function of each mode, in our case defined by Eq. (17) and plotted in Fig. 1. Since this electric field is discrete in the reciprocal space ($M$ modes), it possesses a periodicity length of $L = 2\pi/\Delta k$, where $\Delta k = k_i - k_{i-1}$ is the constant interval of $k$ discretization. In Secs. III B and III C turbulence refers to a large number of overlapping modes, with random phases, of the electric field.

Figure 2(a) shows, in the case of Langmuir dispersion, an example of the autocorrelation function, which corresponds to the integrand term in Eq. (13), plotted as a function of the displacement in time $t$ and space $x$, for a discrete spectrum with $M = 201$ modes. The black dashed diagonal with equation $x = v_{0,\max} t$ is shown in Fig. 2(a); note that $v_{0,\max}$ corresponds to the velocity of maximum-diffusion, which will be discussed later in this section; graphically it aligns with the monotonous curve of origin $(x = 0, t = 0)$. Figure 2(b) shows different autocorrelation functions at different velocities as a function of

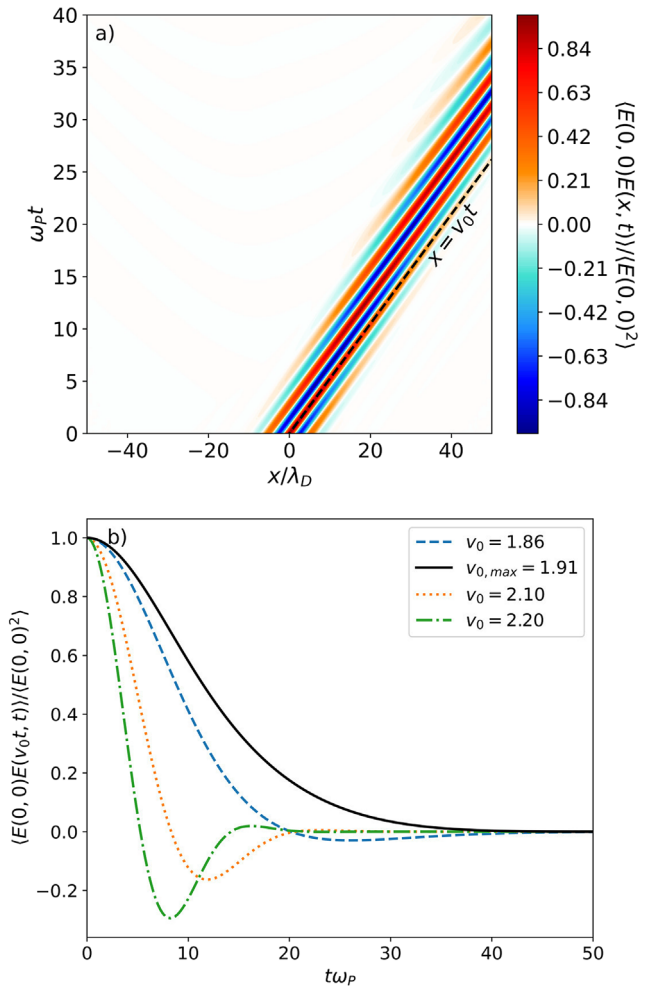


**FIG. 2.** Correlation function of the electric field with Langmuir dispersion and for a spectrum with parameters $k_0 = 1$, $\delta k = 0.4$, $M = 201$, and $a_0 = 8.0 \times 10^{-4}$. (a) Correlation as a function of time and distance, dashed diagonal line for $x = v_{0,\max} t$, where $v_{0,\max}$ corresponds to the velocity where QL diffusion is maximal and (b) correlations functions at $x = v_0 t$ for different velocities $v_0$.

time, in particular the maximum-diffusion autocorrelation (black solid line). As observed in both figures, the autocorrelation function is a smooth, continuous, and non-monotonic function (only for $v_{0,\max}$ the function is monotonic), which converges to zero for large values of the time. These properties allow for simple numerical integration and, therefore, calculation of diffusion coefficients, Eq. (13).

Since the electric field is periodic, the autocorrelation function also presents a periodicity in both space and time directions called echoes. In our case, we chose the number of modes and spacing $\Delta k$ such that these echoes are located far apart and do not interfere with the integration of the autocorrelation function. Moreover, as shown in the previous Sec. II C, we calculate the diffusion coefficients by integrating the autocorrelation function over time. Numerically, we transform the indefinite integral to a definite integral with a finite upper bound as long as the autocorrelation goes to zero after a few $\omega_p^{-1}$, which is the

case for Langmuir and ion-acoustic dispersion relations [shown in Fig. 2(b) for Langmuir dispersion].

To compare against theory, we study the dynamics of test particles in the prescribed turbulent electric field. We developed an algorithm that calculates $N$ particle trajectories using a fourth-order Runge–Kutta algorithm in the prescribed electric field. At $t=0$, $N$ test particles are initialized with random velocities $v_{0,i}$ and positions $x_{0,i}$. Notably, particle velocities are distributed in a narrow Gaussian probability around a mean velocity $v_0$. Particle positions are distributed uniformly in one periodicity interval of the electric field $[0; L[$. Every time step, trajectory diagnostics are computed, such as particle distributions, statistical moments, and the maximum finite-time Lyapunov exponents.

For each simulation, two quantities are computed: The velocity-diffusion coefficient $D$ by measuring the initial slope of the velocity variance $\sigma_v^2$, and the $p$ parameter of Eq. (10) by measuring the time dependence of the spatial variance $\sigma_x^2$. More details are given in Appendix B.

First, we focus on the quasi-linear theory regime for Kubo number $K \ll 1$. We select three different electric field amplitudes $a_0$, corresponding to $K = [1.3\times10^{-2}, 7.3\times10^{-2}, 1.3\times10^{-1}]$, where $\tau_0 = 12.9\omega_p^{-1}$ and $\tau_0 = 13.1\omega_p^{-1}$ are the Lagrangian autocorrelation time of the electric field at $v_{0,\max}$ calculated from Eq. (2), for the Langmuir and ion-acoustic dispersion, respectively. The typical resonance broadening time at $v_{0,\max}$ for the three values of Kubo and the Langmuir dispersion relation are $\tau_{RB}\omega_p \sim [551, 56, 26]$. We perform a series of simulations for each dispersion relation at different particle mean velocities $v_0$.

Figure 3 shows the numerical $p$ parameter against velocities for the Langmuir set of simulations. First, we observe that this $p$ parameter is not constant over particle velocities for the three values of the Kubo number, and it takes values varying around $p=3$, which corresponds to the asymptotic value of $p$ for large enough times.[10,14] The dashed curves in Fig. 3 show the smoothed out distribution function of $p$ used to compute the analytical resonance broadening diffusion coefficients in Eq. (14).

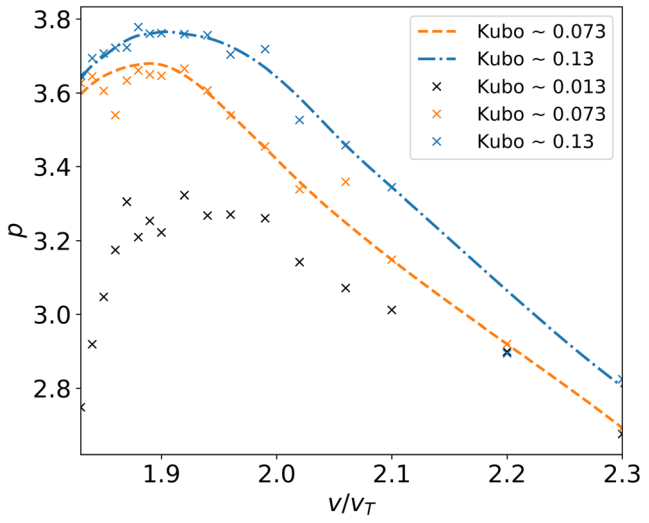


**FIG. 3.** The resonance broadening $p$ parameter distribution as a function of particle velocity for three values of Kubo number, Gaussian amplitude, and Langmuir dispersion relation.

The analytical quasi-linear and resonance broadening diffusion is compared against diffusion from numerical simulations in Figs. 4(a) and 4(b), for Langmuir and ion-acoustic dispersion simulations, respectively. We find qualitative and quantitative agreement between theory and numerical results for the two dispersion relations and the three values of the Kubo number.

Note that for $K \leq 1.3\times10^{-2}$, the numerical and resonance broadening diffusion coefficients converge to the quasi-linear diffusion coefficient. On the other hand, resonance broadening effects become significant for Kubo of a few percent ($K \simeq 7.3\times10^{-2}$, which

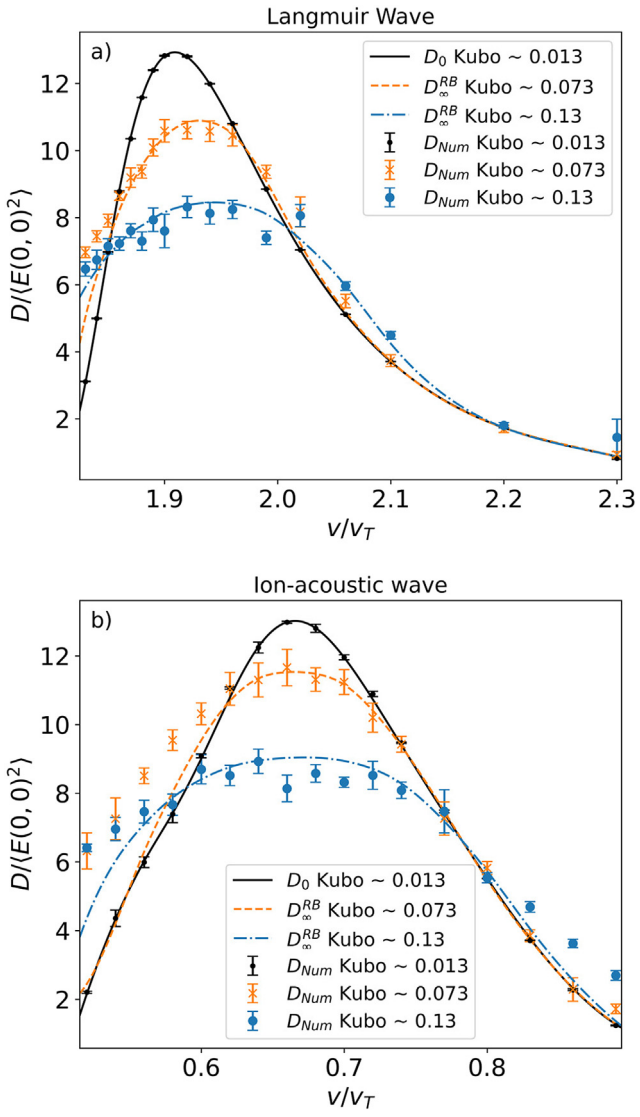


**FIG. 4.** Comparison of analytic (solid, dotted, and dashed lines) and numerical (points, crosses, and stars) diffusion coefficients as a function of the initial velocity of particles $v$ for three different initial electric field amplitudes. (a) Simulations with Langmuir dispersion relation and (b) with ion-acoustic dispersion relation.

corresponds to $a_0 \simeq 10^{-3}$ in terms of electric field amplitude). These effects correspond to a flattening of the diffusion curves, an increase in the maximum-diffusion velocity, and an enlargement of the velocity interval where particles diffuse, as explained in Sec. II C. For these Kubo numbers, particles are partially, or fully, trapped in the electric field (see Appendix A for more details), therefore, exploring a wider range of velocities around the initial velocity. These variations result in an increase in the number of waves interacting with the particle, but with a limited, relatively local, range. This leads to an effective average operation on the diffusion felt by particles.

Furthermore, the diffusion coefficients are bell-shaped for the chosen dispersion relations. Indeed, the maximum diffusion, located at $v_{0,\max}$, corresponds to the velocity of maximum resonance between waves and particles. This resonance corresponds to the velocity shown as a diagonal in the autocorrelation function in Fig. 2(a).

From numerical simulations, we observe a broadening and decrease in amplitude of the particle diffusion as expected from resonance broadening theory for Langmuir and ion-acoustic dispersion relations. However, for the ion-acoustic dispersion relation, Fig. 4(b), we observe a difference in diffusion coefficients between resonance broadening theory and numerical simulations. Simulation diffusion is greater than predicted for values at the boundaries of the velocity interval. This effect becomes more noticeable as the Kubo number increases or for less-dispersive waves, such as ion-acoustic waves. This effect is studied in detail in Sec. III C for Langmuir dispersion simulations and high Kubo numbers.

### C. Large Kubo number

For the second study, we have investigated the evolution of the diffusion coefficient outside the validity range of the quasi-linear theory regime. In other words, for Kubo numbers larger than one ($K \geq 1$) with Langmuir dispersion relation. First, we chose two values of the electric field amplitude corresponding to $K \simeq 1.8$ and $K \simeq 4.0$, respectively. The results are shown in Fig. 5. We find that RB theory predicts the order of magnitude of diffusion for velocities around the resonance velocity ($v < 4v_T$), but a significant discrepancy in the shape of the diffusion coefficient is observed. Note that the ratio between the analytical and numerical diffusion coefficients is not constant and depends on simulation parameters. Furthermore, we measure a significant diffusion from numerical simulations for fast particles, while negligible diffusion is predicted by quasi-linear theory and resonance broadening. Finally, we observe that the diffusion coefficients converge regardless of the Kubo number for particle velocities over $v > 8v_T$ and $K > 1$. Indeed, as explained in Subsec. III B, the electric field is discrete and distributed for the most part around the resonance velocity region of $v < 4v_T$, with a small number of modes located at velocities outside this region. Therefore, a small diffusion coefficient is measured for high enough particle velocities where only two chains of islands overlap. Moreover, as the electric field amplitude increases, the overlap of these few modes increases, and particle stochasticity and diffusion increase, pushing the boundaries of the plateau to higher velocities.

Finally, we have studied the dependence of the diffusion coefficient as a function of the Kubo number at fixed $v_0$ in two different time intervals. First, for times of the order of $\tau_0$, Fig. 6 shows the normalized diffusion coefficient from numerical simulations as a function of the Kubo number. We observe three different regimes: For $K \ll 1$,

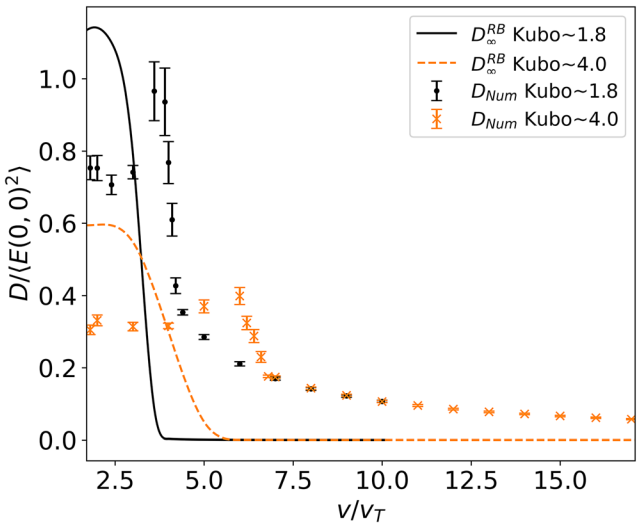


**FIG. 5.** Comparison of analytic (solid, dotted, and dashed lines) and numerical (points, crosses, and stars) diffusion coefficients as a function of the initial velocity of particles $v$ for Kubo number of 1.8 and 4.0, with Langmuir dispersion relation.

the normalized diffusion is constant as predicted by quasi-linear theory. This is followed by a transition regime where the Kubo number is of the order of a few percent; here, the diffusion coefficient decreases non-linearly as observed in Subsec. III B and predicted by resonance broadening.[14,15] For the case of $K > 0.5$, the normalized diffusion evolves as a power of the Kubo number $K^{-1}$. Similar results are found for ion-acoustic dispersion relation.

As of the writing of this article, there is no theory or method to predict diffusion in the large Kubo regime accurately. Nevertheless, we observed particle trajectories to resemble those originating from a

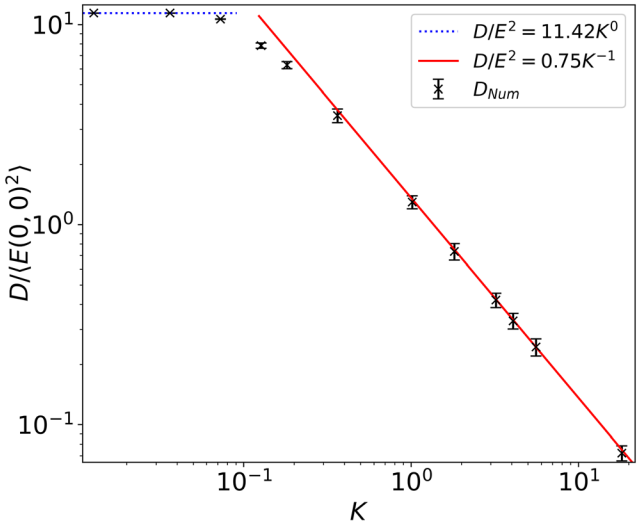


**FIG. 6.** Numerical diffusion coefficient in crosses as a function of the Kubo number $K$, for $v_0 = 1.95$. The power law fit dependence on Kubo number of diffusion is in solid and dashed lines.

random walk of the centers of trapped-particle trajectories in velocity space. Therefore, we suppose that the diffusion coefficient takes the form $D = \frac{\Delta v^{RW}}{2\Delta t}$. Here, we define the elapsed time between jumps as $\Delta t = \tau_b$, the time for a particle to perform one trapped orbit. We define the velocity step to be the resonance broadening[10] $\Delta v^{RW} = \Delta v^{TB} = (D/6k)^{1/3}$, which corresponds to the range of velocities that particles can interact with neighbor electrostatic modes. This approximation shows that for $K \gg 1$, diffusion scales as a power of the electric field: $D = CE^{3/2}$, where $C = k^3/288$, matching the results of Fig. 6. Note that this expression predicts the proper electric field scaling but may not predict the exact value of diffusion. In our case, by denormalizing the diffusion coefficient and using the second expression of the Kubo number, $K \propto E^2$, our results become: In the quasi-linear regime, $D$ is proportional to $K^4 \propto E^2$, and for large Kubo numbers, $D$ is proportional to $K^3 \propto E^{3/2}$.

Finally, we studied the second slope on $\sigma_v^2$ located at times much larger than $\tau_b$ and $\tau_0$ (see Subsec. 2 of Appendix B). In this regime, we measure the first four statistical moments and the maximum finite-time Lyapunov exponent (FTLE)[42–44] to characterize the second slope on $\sigma_v^2$. First, in the FTLE diagnostic, we observe that for times of the order of a couple $\tau_b$ (less than $500\omega_p^{-1}$), the FTLE is positive, and it converges to a plateau. For larger times, we observe that the FTLE starts to decrease with time; this gives us an upper limit in simulation time. Nonetheless, particle trajectories remain stochastic for times larger than $500\omega_p^{-1}$ since the value of the FTLE remains positive and, in particular, one-two orders of magnitude higher than for the initial FTLE. Furthermore, by examining particle statistics and distribution, we observe that the excess kurtosis becomes important compared to the variance at larger times. Moreover, the particle distribution becomes non-Gaussian after the time corresponding to the first slope [see Fig. 9(a)]. Thus, this indicates that for longer times, particles do not follow what can be strictly defined as a diffusion despite measuring a slope on $\sigma_v^2$, or in other words, a Hurst parameter of $H \sim 0.5$. Therefore, we name this quantity the slope coefficient $S$.

In Fig. 7, we show the normalized slope coefficient as a function of the Kubo number. First, we observe that $S$ is several orders of magnitude smaller than in the previous Fig. 6, and we observe two different regimes where $S$ evolves as a power of the Kubo number, a first at a relatively low Kubo number, $K < 0.5$, where $S \propto K^{5/2} \propto E^{5/4}$, and a second for a larger Kubo number, $K > 0.5$, where $S \propto K^{3/2} \propto E^{3/4}$.

## IV. CONCLUSION

In summary, we investigated the diffusion of charged particles in a prescribed one-dimensional turbulent electric field by means of numerical simulations and quasi-linear theory. We measured statistical diffusion coefficients at different Kubo number values using a Gaussian amplitude spectrum and realistic plasma dispersion relations: Langmuir and ion-acoustic dispersions. First, diffusion at a low Kubo number was investigated as a function of the initial particle velocity. The results from numerical simulations are in qualitative and quantitative agreement with quasi-linear theory, including resonance broadening as well as with previous papers,[14,15] which studied diffusion at low Kubo numbers and for non-physical dispersion relations. Second, an in-depth study of diffusion coefficients outside the quasi-linear regime, large Kubo numbers, was performed as a function of the Kubo number, where we measured diffusion to scale as a power law, $K^3 \propto E^{3/2}$, which we explain to be a random walk diffusion of the centers of trapped-particle trajectories in the velocity direction. Finally, for times much larger than $\tau_0$ and $\tau_b$, we measure two power laws for the evolution of the slope coefficient $S$ in the form of $K^{5/2} \propto E^{5/4}$ and $K^{3/2} \propto E^{3/4}$ for small and large Kubo number, respectively.

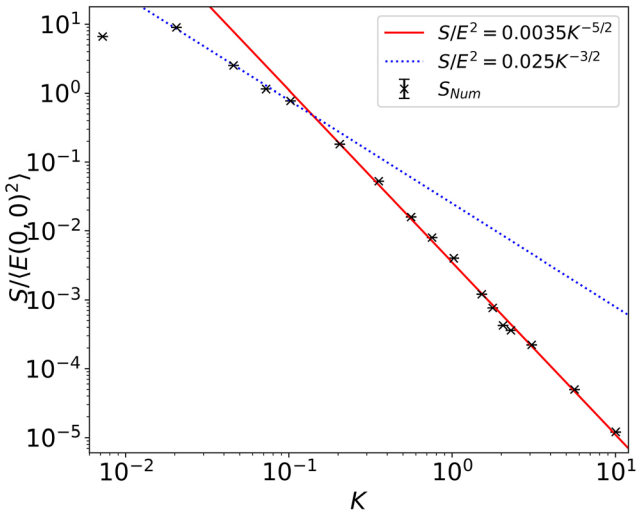


**FIG. 7.** Numerical $S$ coefficient in crosses as a function of the Kubo number $K$ after a time much larger than $\tau_0$, for $v_0 = 1.95$. The power law fit dependence on Kubo number of diffusion is in solid and dashed lines.

In conclusion, in the case of realistic plasma dispersion relations and a prescribed turbulent electric field, quasi-linear and resonance-broadening theories in the limit of small Kubo numbers ($K < 10\%$) accurately predict particle diffusion. Remarkably, a simple random walk expression ($D \propto E^{3/2}$), generally employed in other conditions, predicts the evolution for large Kubo numbers $K \gg 1$. However, further work is required to improve the understanding of turbulence, transport, and diffusion. This study is subject to two caveats: First, the incorporation of the Poisson equation to get a complete self-consistent problem where particle distributions are allowed to modify the electric field, and second, by considering the evolution of phase-space structures.[30,45–50] Consequently, the next step of this study is to consider phase-space structures by prescribing a relationship between the initial phases of the electric field modes, as observed in laboratory plasmas,[19–21] and studying the self-consistent kinetic problem through the Vlasov–Poisson code COBBLES.[50]

## ACKNOWLEDGMENTS

This work was funded by the Agence Nationale de la Recherche for the Project GRANUL (ANR-19-CE30–0005). This work was granted access to the HPC resources of EXPLOR (Project No. 2017M4XXX0251) and CINECA MARCONI under Project FUA35 GSNTITE. This work has been carried out within the framework of the EUROfusion Consortium, funded by the European Union via the Euratom Research and Training Programme (Grant Agreement No. 101052200—EUROfusion). Views and opinions expressed are, however, those of the author(s) only and do not necessarily reflect those of the European Union or the European Commission. Neither the European Union nor the European Commission can be held responsible for them.

## AUTHOR DECLARATIONS

### Conflict of Interest

The authors have no conflicts to disclose.

### Author Contributions

**Alejandro Guillevic:** Conceptualization (equal); Data curation (equal); Formal analysis (equal); Investigation (equal); Methodology (equal); Software (equal); Validation (equal); Visualization (equal); Writing – original draft (equal). **Thierry Reveille:** Writing – review & editing (supporting). **Maxime Lesur:** Conceptualization (equal); Funding acquisition (equal); Methodology (equal); Project administration (equal); Resources (equal); Supervision (equal); Writing – review & editing (equal). **Xavier Garbet:** Writing – review & editing (equal). **Patrick Diamond:** Writing – review & editing (equal). **Guillaume Lo-Cascio:** Methodology (supporting); Writing – review & editing (supporting). **Yusuke Kosuga:** Writing – review & editing (supporting). **Etienne Gravier:** Writing – review & editing (equal). **Debraj Mandal:** Visualization (supporting); Writing – review & editing (supporting). **Alain Ghizzo:** Writing – review & editing (supporting).

## DATA AVAILABILITY

The data that support the findings of this study are available from the corresponding author upon reasonable request.

## APPENDIX A: TEST PARTICLES IN A PRESCRIBED TURBULENT ELECTRIC FIELD

### 1. Single particle trajectories and trapped particle time

In a simple sinusoidal electric field, the movement of a charged particle is known to be an oscillation in time and space. This trajectory can be represented in phase space (x,v) as either closed trajectories or oscillating open trajectories, named *Trapped particles* and *Passing particles*, respectively. Since trapped particle trajectories are closed in phase space, one can define a characteristic time/frequency for which it takes a particle to complete one orbit $\tau_b/\omega_b$, named bouncing time/frequency. A simple expression of the bouncing time for deeply trapped particles is defined as a function of the wave number and electric field amplitude ($k$ and $E$) as

$$\tau_b = 2\pi\sqrt{\frac{m}{|q|kE}}, \tag{A1}$$

and the corresponding bouncing frequency $\omega_b = 2\pi/\tau_b$. In the case of this paper, the electric field is expressed as a sum of sinusoidal waves; therefore, we chose a definition of bouncing time/frequency where the product $kE$ from Eq. (A1) is replaced by $\langle k^2 E(0,0)^2\rangle^{1/2}$. Note that alternatively one can use $k\langle E(0,0)^2\rangle^{1/2}$ where $k$ is either the average wave number ($k = k_0$) or the wave number from the resonant mode ($k = k_j$); however, for the values used in this paper, these only give variations on the bouncing time of less than 15%.

Two examples of test particle trajectories in turbulent electric fields of low and high amplitudes, respectively, shown in Figs. 8(a) and 8(b). As prescribed by quasi-linear theory, trajectories in a low amplitude electric field (small Kubo number), Fig. 8(a), follow Brownian-like motion in phase-space. On the other hand, in a large amplitude field (large Kubo number), Fig. 8(b), particles are trapped in potential wells and follow closed orbits in phase-space, which get disrupted occasionally when particles jump to a neighbor potential well, reminiscing of random-walk motion of the centers of trapped-particle trajectories. Nevertheless, on average, particle trajectories are randomized after several bounce times $\tau_b$ due to the turbulent field. This randomization allows us to calculate statistics on particle trajectories such as statistical moments, the maximum finite-time Lyapunov exponents (FTLE), and in the case of our study, diffusion coefficients.

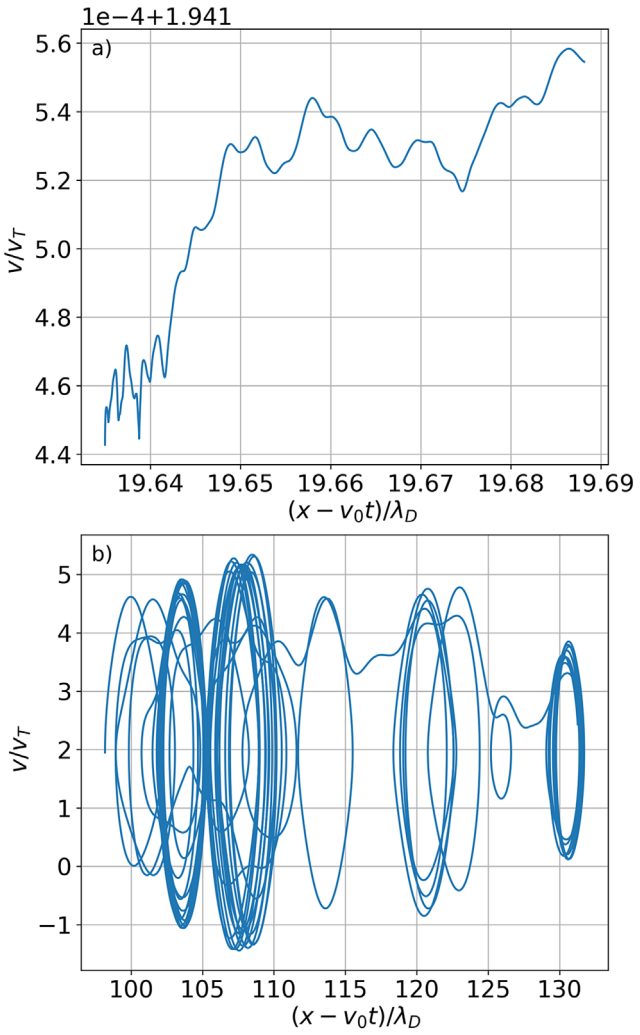


**FIG. 8.** Example of particle trajectories in the wave reference frame $x_i - v_{0,i}t$ and $v_i$ for a small $K = 1.3 \times 10^{-3}$ (a) and large $K = 4.0$ (b) Kubo number.

### 2. Statistics on particle trajectories

As stated in Sec. III B during a simulation, our code calculates different statistical quantities, particularly the first four velocity moments (Mean difference, variance, skewness, and kurtosis), the

spatial and velocity distributions, the FTLE, and the standard velocity deviation $\sigma_v^2$ of Eq. (6). In particular, the first three quantities (moments, distribution, and FTLE) allow us to determine the regime of transport particles follow in the turbulent electric field.

For the transport generated by the electric field to be considered to be diffusion, these quantities should respect some rules:

First, the FTLE can tell us if the transport is stochastic if, in the limit of long times ($t \to +\infty$), the exponent is positive. In this paper, we define the FTLE as[43]

$$\lambda = \frac{1}{t_n - t_0} \sum_{i=1}^{n} \ln\left(\frac{d(t_i)}{d_0}\right), \tag{A2}$$

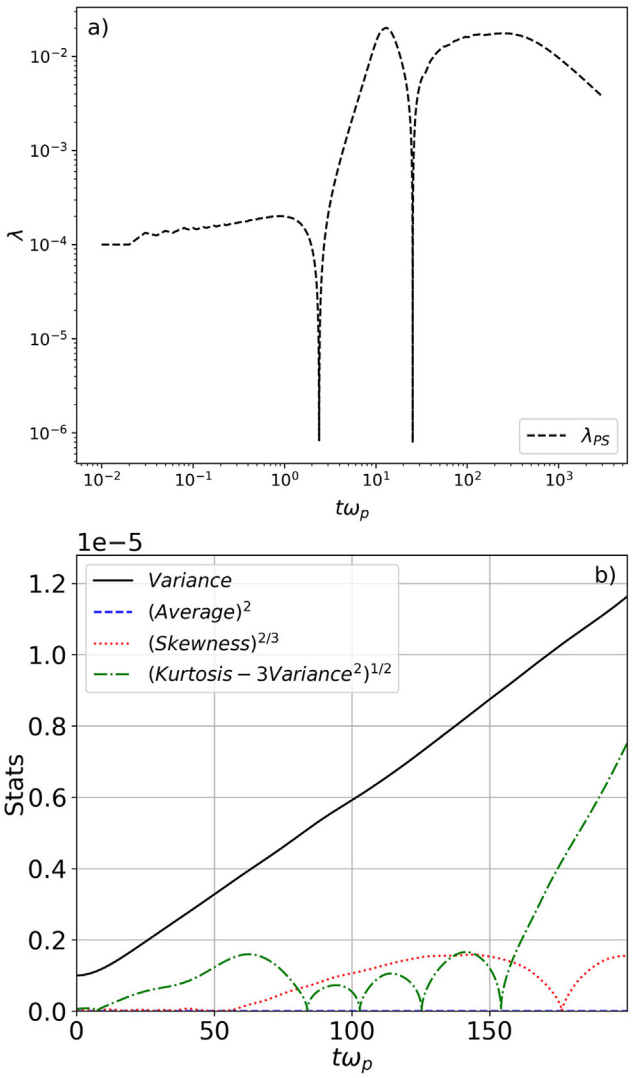


**FIG. 9.** Plots of the maximum finite-time Lyapunov exponent in (a), and the first four statistical moments in (b), for an arbitrary simulation with $N = 480\,000$ test particles.

where $d_0$ and $d(t_i)$ are the distance separating two trajectories at $t = 0$ and $t = t_i$, respectively. Figure 9(a) shows the FTLE as a function of time. For short and intermediary times, $\lambda_{PS}$ is positive and grows until it reaches a maximum where it remains for a couple of $\tau_b$. This is followed by a decrease in the FTLE for large times, outside the time scales of any simulation performed in this paper. Consequently, we can consider particle trajectories as stochastic in the initial time interval, where the FTLE is finite and positive. However, after $t\omega_p \sim 500$, $\lambda_{PS}$ decreases and seems to converge to a negative power of time; however, it remains one-two orders of magnitude larger than the initial FTLE. Therefore, we can consider that particle trajectories remain stochastic for simulation times larger than $500\omega_p^{-1}$.

Second, since particles are initialized with a Gaussian velocity distribution around $v_0$, a pure, homogeneous diffusion will only lead to an increase in particle distribution variance, while the other moments should stay null. However, since diffusion is a function of particle velocity [Eqs. (13) and (14)], one would expect the development of an asymmetry in the distribution of particles, increasing the amplitude of moments other than the variance. Nevertheless, if these moments remain small with respect to the variance, and as long as the standard deviation remains much smaller than the scale of variation of $D(v)$ then the transport generated by the electric field can be considered as a diffusion. Figure 9(b) shows the evolution of the first four velocity moments as a function of time for an arbitrary simulation with a small Kubo number (The same results are found for a large Kubo number). We observe that at the start of the simulation, the variance remains considerably larger than the other three moments, until at $t\omega_p = 155$, the kurtosis increases and becomes significant.

Hence, the transport generated by a turbulent electric field of the form presented in Sec. III A leads to the stochastic diffusion of particles in a time interval of several $\tau_0$. For later times, we cannot guarantee that the transport is diffusive.

## 3. Chirikov overlap criterion

The Chirikov parameter or Chirikov resonance-overlap criterion[51] measures the ratio of superposition of two neighboring waves to characterize the chaotic motion in deterministic Hamiltonian systems. Mathematically it is defined as

$$\Lambda = \frac{\Delta^{1/2} v_i + \Delta^{1/2} v_{i+1}}{\Delta v_{i,i+1}^{\phi}}, \tag{A3}$$

where $\Delta^{1/2} v_i = \sqrt{\frac{2qE_i}{mk_i}}$ is half of the maximum width of the separatrix along the velocity direction; here, $E_i$ and $k_i$ are the $i$th mode electric field amplitude and wave number, and $\Delta v_{i,i+1}^{\phi}$ is the difference between the $i$ and $i+1$ modes phase velocities.

For regular dynamics, the Chirikov criterion takes values much lower than unity $\Lambda \ll 1$, and for chaotic dynamics $\Lambda \geq 1$. For values closer to unity, $\Lambda \lesssim 1$, the width of the chaotic domain in phase space is smaller compared to the case where it is $\Lambda \gtrsim 1$. For example, at $\Lambda = 0.5$, the chaotic region will be narrow and localized near the separatrix, and for $\Lambda > 1$, the chaotic region will become significant, encompassing the whole domain.

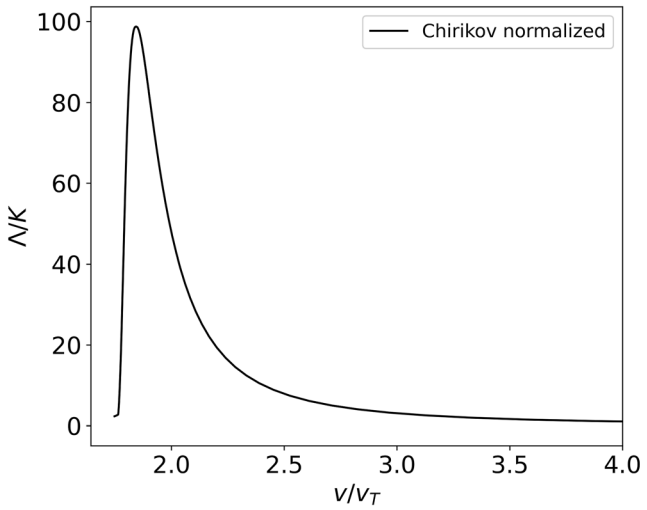


**FIG. 10.** Velocity distribution of the local Chirikov overlap criterion $\Lambda$, normalized to the Kubo number $K$.

Figure 10 shows the velocity distribution of the local Chirikov overlap criterion normalized to the Kubo number. We choose to normalize the Chirikov criterion by the Kubo number since, for two arbitrary waves, the numerator is proportional to the square amplitude of the electric field, in other words, $\Delta^{1/2}\nu_i \propto \sqrt{E}$ which is the same dependence as the Kubo number $K \propto \sqrt{E}$. Note that the Chirikov distribution is comparable to the QL diffusion coefficient of Fig. 4(a); it is a bell-shape function with a maximum at $v \sim 1.9v_T$ and a tail that approaches zero as $v/v_T$ increases.

## APPENDIX B: MEASUREMENT OF DIFFUSION COEFFICIENT AND *P* PARAMETER

### 1. Resonance broadening *p* parameter

In resonance broadening theory, the $p$ parameter describes the evolution of the position standard deviation as the $p$ power function of time, defined in Eq. (10). Analytically, $p$ is expected to converge to $p=3$ when $t \to +\infty$. Indeed, Dupree[10] shows in Eq. (7.1) that for the self-consistent kinetic problem, $p=3$ is a solution. Moreover, Doveil and Grésilion[14] define the asymptotic $p$ as such. However, a measurement of $\sigma_x^2$ from numerical simulations was not performed.

In our simulations, we observed the $p$ parameter to fluctuate in the interval $]2,4[$ and indeed for large enough times to converge to $p=3$. However, the diffusion regime of a simulation is located in the time interval of several $\tau_0$, as shown in Subsec. 2 of Appendix A. Therefore, we measured and characterized the $p$ parameter for different Kubo numbers and initial velocities. The results are plotted in Fig. 3.

We smoothed out the numerical distribution of $p$ (shown in dashed lines) for the analytical resonance broadening diffusion coefficient calculation. This methodology allows us to use resonance broadening in the diffusion regime and compare it against numerical results. Furthermore, as presented in Subsec. III B, we have a qualitative and quantitative agreement between numerical results and theory for the Kubo number of a few percent.

### 2. Diffusion estimation: $\sigma_v^2$ slope measurement

As written in Eq. (7), a diffusion coefficient is defined as the slope of the velocity variance $\sigma_v^2$. Therefore, we estimate diffusion coefficients by measuring the linear slope of $\sigma_v^2$ over a dozen of $\tau_0$. Figures 11 and 12 show the velocity variance $\sigma_v^2$ for a small, medium, and large Kubo number in a solid black line and the linear slope in red dashed line.

Three phases can be observed in the evolution of $\sigma_v^2$: In the first phase, where $\sigma_v^2$ evolves parabolically. After around one $\tau_0$, a second phase of variable length starts where $\sigma_v^2$ grows linearly. Here

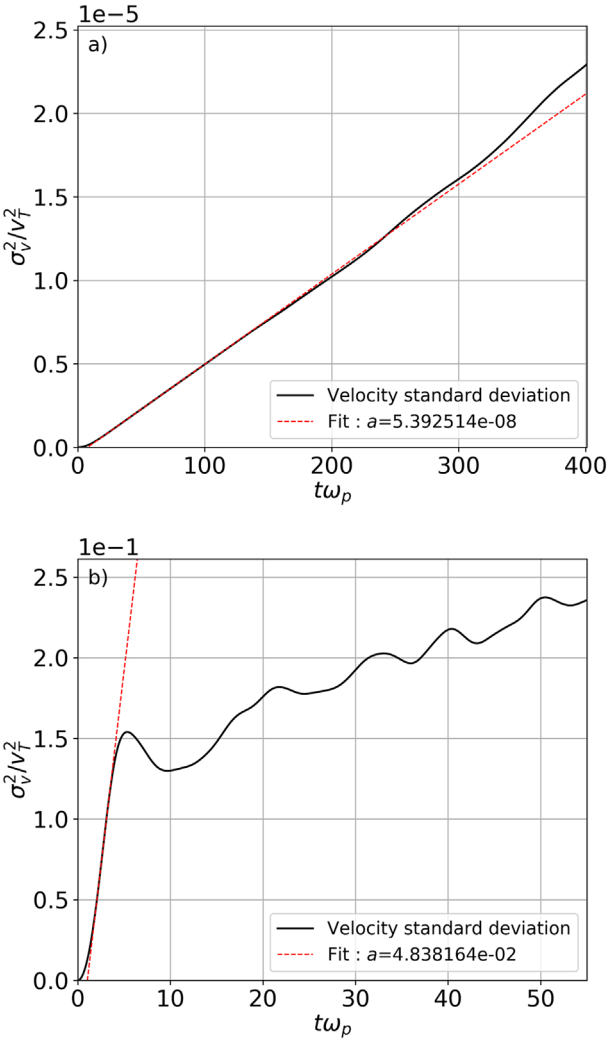


**FIG. 11.** In solid lines, the velocity standard deviation as a function of time for two arbitrary simulations with Langmuir dispersion, and in the red dashed line, the linear fit in the diffusion regime. In (a) with Kubo number $K = 1.3 \times 10^{-2}$ and in (b) with Kubo number $K = 1.3$.

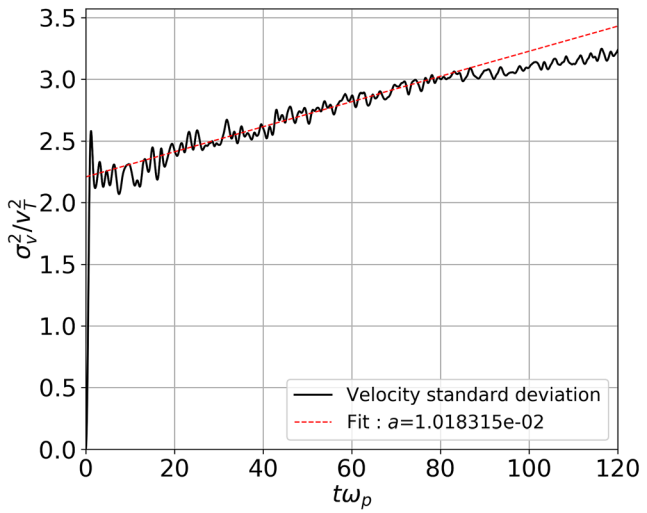


**FIG. 12.** In solid line, velocity standard deviation of a typical simulation with Langmuir dispersion at Kubo number $K = 2.7$. The red dashed line is the linear fit during the second slope regime.

diffusion is estimated by the measurement of the linear slope in this time interval. Finally, a third phase begins when the first slope of $\sigma_v^2$ changes amplitude drastically. However, due to previous arguments, this quantity statistically cannot be equated to a diffusion coefficient.

## REFERENCES


[1]A. N. Kolmogorov, "The local structure of turbulence in incompressible viscous fluid for very large Reynolds numbers," Akad. Nauk SSSR Dokl. **30**, 301–305 (1941).
[2]J. B. Mcbride, O. T. Edward, J. P. Boris, and J. H. Orens, "Theory and simulation of turbulent heating by the modified two-stream instability," Phys. Fluids **15**, 2367–2382 (1972).
[3]R. J. Hamilton and V. Petrosian, "Stochastic acceleration of electrons. I—Effects of collisions in solar flares," Astrophys. J. **398**, 350 (1992).
[4]W. Liu, V. Petrosian, B. R. Dennis, and Y. W. Jiang, "Double coronal hard and soft x-ray source observed by RHESSI: Evidence for magnetic reconnection and particle acceleration in solar flares," Astrophys. J. **676**, 704–716 (2008).
[5]L. M. Gorbunov, "Hydrodynamics of plasma in a strong high-frequency field," Sov. Phys. Usp. **16**, 217 (1973).
[6]V. Y. Bychenkov, "Ion acoustic turbulence driven by return current leads to hot electrons in laser-produced plasma," Phys. Plasmas **25**, 102706 (2018).
[7]Y. Romanov and G. F. Filippov, "The interaction of fast electron beams with longitudinal plasma waves," Sov. Phys. JETP **13**, 87–92 (1961).
[8]W. Drummond and D. Pines, "Nonlinear stability of plasma oscillations," Nucl. Fusion **3**, 1049–1057 (1962).
[9]A. A. Vedenov, E. P. Velikhov, and R. Z. Sagdeev, "Quasilinear theory of plasma oscillations," Nucl. Fusion **2**, 465–475 (1962).
[10]T. H. Dupree, "A perturbation theory for strong plasma turbulence," Phys. Fluids **9**, 1773 (1966).
[11]J. Weinstock, "Turbulent diffusion, particle orbits, and field fluctuations in a plasma in a magnetic field," Phys. Fluids **11**, 1977–1981 (1968).
[12]J. C. Adam, G. Laval, and D. Pesme, "Effets des interactions résonnantes ondes-particules en turbulence faible des plasmas," Ann. Phys. **6**, 319–420 (1981).
[13]G. Laval and D. Pesme, "Breakdown of quasilinear theory for incoherent 1-D Langmuir waves," Phys. Fluids **26**, 52–65 (1983).
[14]F. Doveil and D. Grésillon, "Statistics of charged particles in external random longitudinal electric fields," Phys. Fluids **25**, 1396–1402 (1982).
[15]A. Hirose and O. Ishihara, "On plasma diffusion in strong turbulence," Can. J. Phys. **77**, 829–833 (1999).
[16]M. Vlad and F. Spineanu, "Random and quasi-coherent aspects in particle motion and their effects on transport and turbulence evolution," New J. Phys. **19**, 025014 (2017).
[17]J. Médina, M. Lesur, E. Gravier, T. Réveillé, M. Idouakass, T. Drouot, P. Bertrand, T. Cartier-Michaud, X. Garbet, and P. H. Diamond, "Radial density and heat fluxes description in the velocity space: Nonlinear simulations and quasi-linear calculations," Phys. Plasmas **25**, 122304 (2018).
[18]K. Lim, E. Gravier, M. Lesur, X. Garbet, Y. Sarazin, and J. Médina, "Impurity pinch generated by trapped particle driven turbulence," Plasma Phys. Controlled Fusion **62**, 095018 (2020).
[19]S. I. Tsunoda, F. Doveil, and J. H. Malmberg, "Nonlinear Interaction between a warm electron beam and a single wave," Phys. Rev. Lett. **59**, 2752–2755 (1987).
[20]S. I. Tsunoda, F. Doveil, and J. H. Malmberg, "Experimental test of the quasi-linear theory of the interaction between a weak warm electron beam and a spectrum of waves," Phys. Rev. Lett. **58**, 1112–1115 (1987).
[21]S. I. Tsunoda, F. Doveil, and J. H. Malmberg, "Experimental test of quasilinear theory," Phys. Fluids B **3**, 2747–2757 (1991).
[22]N. Besse, Y. Elskens, D. F. Escande, and P. Bertrand, "Validity of quasilinear theory: Refutations and new numerical confirmation," Plasma Phys. Controlled Fusion **53**, 025012 (2011).
[23]D. W. Crews and U. Shumlak, "On the validity of quasilinear theory applied to the electron bump-on-tail instability," Phys. Plasmas **29**, 043902 (2022).
[24]R. Kubo, "Stochastic Liouville equations," J. Math. Phys. **4**, 174–183 (1963).
[25]M. Vlad, F. Spineanu, J. H. Misguich, J. D. Reuss, R. Balescu, K. Itoh, and S. I. Itoh, "Lagrangian versus Eulerian correlations and transport scaling," Plasma Phys. Controlled Fusion **46**, 1051–1063 (2004).
[26]D. F. Escande and F. Sattin, "When can the Fokker-Planck equation describe anomalous or chaotic transport?," Phys. Rev. Lett. **99**, 185005 (2007).
[27]P. H. Diamond, S. I. Itoh, and K. Itoh, *Modern Plasma Physics: Physical Kinetics of Turbulent Plasmas* (Cambridge University Press, 2010).
[28]A. Lenard, "On Bogoliubov's kinetic equation for a spatially homogeneous plasma," Ann. Phys. **10**, 390–400 (1960).
[29]R. Balescu, *Statistical Mechanics of Charged Particles* (Interscience, 1963).
[30]T. H. Dupree, "Theory of phase space density granulation in plasma," Phys. Fluids **15**, 334–344 (1972).
[31]B. V. Chirikov, "Research concerning the theory of non-linear resonance and stochasticity," Report No. 267 (Nuclear Physics Institute of Siberian Academy of Sciences, 1969).
[32]B. V. Chirikov, "A universal instability of many-dimensional oscillator systems," Phys. Rep. **52**, 263–379 (1979).
[33]A. B. Rechester, M. N. Rosenbluth, and R. B. White, "Fourier-space paths applied to the calculation of diffusion for the Chirikov-Taylor model," Phys. Rev. A **23**, 2664–2672 (1981).
[34]D. F. Escande, "Renormalization for stochastic layers," Physica D **6**, 119–125 (1982).
[35]R. Z. Sagdeev, *Reviews of Plasma Physics*, edited by A. M. A. Leotovich (Consultants Bureau, New York, 1966), Vol. 4.
[36]T. H. Dupree, "Nonlinear theory of drift-wave turbulence and enhanced diffusion," Phys. Fluids **10**, 1049–1055 (1967).
[37]O. Ishihara, H. Xia, and A. Hirose, "Resonance broadening theory of plasma turbulence," Phys. Fluids B **4**, 349–362 (1992).
[38]D. Bénisti and D. F. Escande, "Finite range of large perturbations in Hamiltonian dynamics," J. Stat. Phys. **92**, 909–972 (1998).
[39]D. Bénisti and D. F. Escande, "Origin of diffusion in Hamiltonian dynamics," Phys. Plasmas **4**, 1576–1581 (1997).
[40]J. R. Cary, D. F. Escande, and A. D. Verga, "Nonquasilinear diffusion far from the chaotic threshold," Phys. Rev. Lett. **65**, 3132–3135 (1990).
[41]L. Boltzmann, *Lectures on Gas Theory*, 1st ed. (Dover Publications, 1895).
[42]J. Brandon, A. J. Lichtenberg, and M. A. Lieberman, Math. Gaz. **79**, 234 (1995).
[43]G. Benettin, L. Galgani, and J. M. Strelcyn, "Kolmogorov entropy and numerical experiments," Phys. Rev. A **14**, 2338–2345 (1976).
[44]M. V. Falessi, F. Pegoraro, and T. J. Schep, "Lagrangian coherent structures and plasma transport processes," J. Plasma Phys. **81**, 495810505 (2015).
[45]I. B. Bernstein, J. M. Greene, and M. D. Kruskal, "Exact nonlinear plasma oscillations," Phys. Rev. Lett. **108**, 546 (1957).

[46]H. L. Berk, C. E. Nielsen, and K. V. Roberts, "Phase space hydrodynamics of equivalent nonlinear systems: Experimental and computational observations," Phys. Fluids **13**, 980–995 (1970).
[47]H. Schamel, "Stationary solutions of the electrostatic Vlasov equation," Plasma Phys. **13**, 491–505 (1971).
[48]H. Schamel, "Non-linear electrostatic plasma waves," J. Plasma Phys. **7**, 1–12 (1972).
[49]H. Berk, B. Breizman, and N. Petviashvili, "Spontaneous hole-clump pair creation in weakly unstable plasmas," Phys. Lett. A **234**, 213–218 (1997).
[50]M. Lesur, P. H. Diamond, and Y. Kosuga, "Nonlinear current-driven ion-acoustic instability driven by phase-space structures," Plasma Phys. Controlled Fusion **56**, 075005 (2014).
[51]B. V. Chirikov, "Resonance processes in magnetic traps," Sov. J. At. Energy **6**, 464–470 (1960).